Mechanobiology

International Edition: DOI: 10.1002/anie.201600351
German Edition: DOI: 10.1002/ange.201600351

Mechanically Induced Catalytic Amplification Reaction for Readout of Receptor-Mediated Cellular Forces

*Victor Pui-Yan Ma, Yang Liu, Kevin Yehl, Kornelia Galior, Yun Zhang, and Khalid Salaita**

Abstract: *Mechanics play a fundamental role in cell biology, but detecting piconewton (pN) forces is challenging because of a lack of accessible and high throughput assays. A mechanically induced catalytic amplification reaction (MCR) for readout of receptor-mediated forces in cells is described. Mechanically labile DNA duplexes presenting ligands are surface immobilized such that specific receptor forces denature the duplex and thus expose a blocked primer. Amplification of primers is achieved using an isothermal polymerization reaction and quantified by fluorescence readout. As a proof of concept, the assay was used to test the activity of a mechanomodulatory drug and integrin adhesion receptor antibodies. To the best of our knowledge, this is the first example of a catalytic reaction triggered in response to molecular piconewton forces. The MCR may transform the field of mechanobiology by providing a new facile tool to detect receptor specific mechanics with the convenience of the polymerase chain reaction (PCR).*

Coupling between mechanical forces and chemistry at interfaces plays a profound role in biological processes, ranging from biofilm formation, to stem cell differentiation and wound healing.[1] To understand these types of chemo-mechanical coupling processes, it is necessary to develop methods to quantify cellular forces. This is challenging because molecular forces in biochemical processes are transient and tend to range from about 1–100 pN, which is sufficient to drive conformational changes in proteins but insufficient to dissociate covalent bonds.[2] Therefore, forces in biochemical systems are difficult to detect and map.

We previously developed molecular tension-based fluorescence microscopy (MTFM) to image forces transmitted by cell surface receptors in living cells.[3] The initial tension probes were comprised of an extendable polyethylene glycol (PEG) spring, flanked by a fluorophore and a spectroscopically matched quencher.[4] Piconewton forces extend the mean end-to-end distance of the polymer, which reduces energy transfer through an R^{-6} distance-dependent relationship. Next generation probes utilized oligonucleotides,[5] elastic polypeptides,[6] and engineered proteins,[7] and also employed gold nanoparticle quenchers to extend energy transfer distances and enhance sensitivity.[7,8]

Nonetheless, the sensitivity of MTFM is limited because of the energy transfer-based readout and the transient nature of cellular forces. For example, current probes require high-end microscopy systems with single-photon counting EMCCDs coupled with high-numerical aperture objectives to detect changes in energy transfer efficiency. Accordingly, high-throughput screening of drugs that target mechanical processes is prohibitive. Likewise, screening the mechanical phenotype of a library of cells is currently a challenge. Therefore, there is a pressing need to develop strategies that transduce piconewton forces into an easily quantifiable, and amplified chemical signal. As a corollary, catalytic amplification strategies, such as PCR and ELISA, provide the foundation of modern molecular and cellular biology. Equivalent assays for mechanics may transform the field of mechanobiology.

Enzymes that respond to specific piconewton mechanical inputs are widespread in nature.[9] In contrast, synthetic systems that transduce defined piconewton forces into a catalytic output are rare (Scheme 1 A). To the best of our knowledge, the only examples of synthetic catalytic reactions that are mechanically triggered are based on polymer structures that initiate mixing of an enzyme and its substrate.[10] These systems are sensitive to bulk forces, measured in units of kPa, rather than molecular piconewton events.

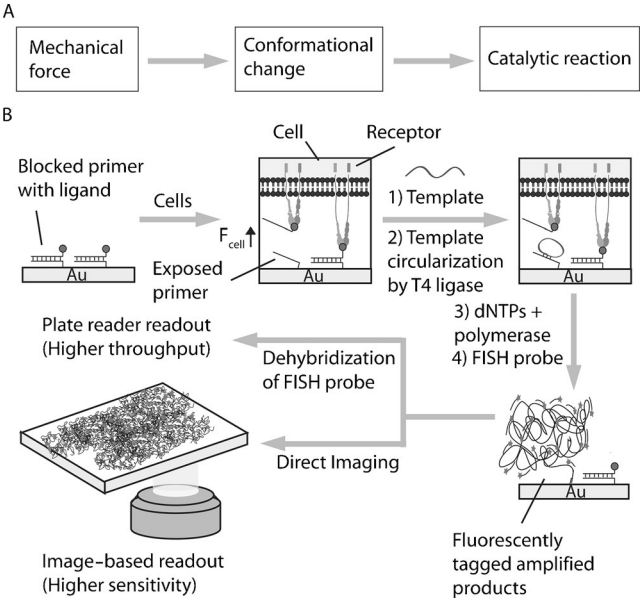

Scheme 1. The mechanically induced catalytic amplification reaction.

[*] V. P.-Y. Ma, Y. Liu, Dr. K. Yehl, K. Galior, Y. Zhang, Prof.Dr. K. Salaita
Department of Chemistry, Emory University
Atlanta, GA 30322 (USA)
E-mail: k.salaita@emory.edu
Prof.Dr. K. Salaita
Wallace H. Coulter Department of Biomedical Engineering, Georgia Institute of Technology and Emory University
Atlanta, GA 30322 (USA)

Supporting information for this article can be found under: http://dx.doi.org/10.1002/anie.201600351.

Herein, we present the mechanically induced catalytic amplification reaction (MCR) to readout the signal associated with piconewton forces applied by cell surface receptors. The strategy depends on a blocked initiator of an enzymatic reaction that is exposed through the action of mechanical forces. Given the fidelity and sensitivity of PCR, we aimed to leverage DNA amplification as a proof of concept readout for MCR. The mechanically responsive element was a DNA duplex inspired by a tension gauge tether (TGT) assay developed by Wang and Ha.[11] In the TGT assay, an immobilized DNA duplex denatures in response to cellular forces exceeding the tension tolerance, T_{tol} (defined as the minimum force needed to denature DNA when applied for 2 s). TGTs are a powerful tool for defining the mechanical forces needed for receptor activation.

As illustrated in Scheme 1 B, a DNA duplex modified with a ligand is surface immobilized. When cells are plated on the surface, adhesion receptors engage their ligands and apply mechanical forces ($F_{receptor}$). Receptor-mediated tension exceeding the T_{tol} exposes the blocked primer for amplification. We demonstrate MCR using isothermal amplification (rather than PCR) to minimize background arising from thermal denaturation of the blocked primer. For amplification, an 81-mer linear DNA template is hybridized and circularized by T4 ligase (Supporting Information, Table S1 for DNA sequences). Subsequently, the primer strand is replicated with isothermal rolling circle amplification (RCA).[12] Under optimal conditions, the RCA reaction replicates a circular template thousands of times, generating a long tandem repeat of DNA (Supporting Information, Figure S1). The repetitive amplified product is then visualized by fluorescence in situ hybridization (FISH), an established technique for sensitive nucleic acid detection with high specificity.[13] Quantification of the product can be achieved by direct surface imaging, or by release of fluorescent oligonucleotides followed by high-throughput plate reader measurements (Scheme 1 B). In principle, each mechanical rupturing event is transduced and amplified into hundreds of fluorescent oligonucleotides.

Immobilization imposes a steric constraint on polymerases, therefore we first quantified the efficiency and selectivity of RCA on a surface. 5′-Thiol modified primers with a T_{10} spacer were immobilized onto gold films[14] and amplified, as described in Scheme 1 B. Surface imaging of hybridized FISH probes in the amplified samples revealed a fluorescent monolayer with a $15.7 \pm 4.9\,\%$ coefficient of variation (CV) in intensity (Figure 1 A), which is likely because of heterogeneous efficiency of polymerization on the surface. In contrast, the non-amplified samples showed a $4.9 \pm 0.3\,\%$ CV, demonstrating that the hybridization of the complement to the primer strand is relatively more homogeneous. Importantly, the fluorescence signal in the amplified primer samples showed a 102 ± 4-fold increase compared to non-amplified samples (Figure 1 B). Solution amplification shows approximately 1000-fold replication of the circular template, as determined by gel electrophoresis (Supporting Information, Figure S1),[12a] thus surface confinement inhibits polymerase activity and reduces the overall amplification efficiency. The roughly 100-fold enhancement in signal

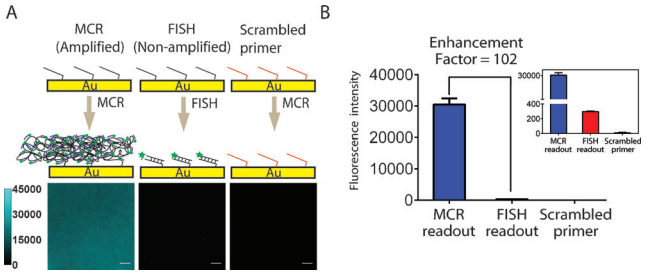

Figure 1. Selectivity and efficiency of surface initiated isothermal amplification. A) Schematic and representative epifluorescence images; B) plot of mean signal from positive (primer), and negative controls (non-amplified sample, and scrambled primer). Error bars represent S.E.M. obtained from three independent experiments (total 30 images). Scale bars = 10 μm.

represents the maximum amplification of a mechanically triggered dehybridization event into a chemical output.

Subsequently, MCR was used to detect forces mediated by integrins, which are a family of heterodimeric cell surface receptors that mediate cell adhesion and migration. Integrins physically bridge the cellular cytoskeleton with the extracellular matrix, and accordingly experience piconewton forces.[15] Assays that allow for screening of compounds that modulate integrin tension are potentially significant.

First, we quantified integrin-mediated denaturation of immobilized DNA duplexes. 5′-Cy3B, 3′-biotin labeled complement was hybridized to the primer to generate a fluorescently labelled duplex (Figure 2 A). Biotin-streptavidin binding was used to present the cyclic Arg-Gly-Asp-D-Phe-Lys (cRGDfK) peptide, a high-affinity ligand for integrin receptors. In this geometry, mechanical forces denature the duplex in an unzipping mode with a predicted $T_{tol} = 12$ pN. An identical primer sequence hybridized to a complement with 3′-Cy3B, 5′-biotin, leads to denaturation in a shearing mode with a predicted $T_{tol} = 56$ pN. Note that the surface presents chemically identical probes with differing mechanical tolerance. After plating NIH/3T3 fibroblast cells on these surfaces for 1 h, we observed a loss in fluorescence that colocalized with the cell footprint, as indicated by reflection interference contrast microscopy (RICM; Figure 2 B). Minimal loss in fluorescence was observed when the cRGDfK adhesion peptide was withheld (not shown). We quantified the decrease in Cy3B fluorescence under individual cells (Figure 2 C) and found that a greater fraction of the $T_{tol} = 12$ pN duplexes were denatured ($13.7 \pm 0.9\,\%$ decrease in fluorescence) compared to that of the $T_{tol} = 56$ pN duplex ($6.5 \pm 0.45\,\%$ decrease in fluorescence). The data shows differential mechanical denaturation of DNA duplexes, with a two-fold difference in DNA loss when comparing the 12 pN to 56 pN duplexes.

To catalytically amplify exposed primers, we plated 100 000 cells to the 12 and 56 pN surfaces (surface area = 68.58 mm^2) and allowed them to spread for 1 h. This cell density corresponds to a full monolayer (680 μm^2 available per cell, assuming each cell can spread ca. 900 μm^2). We then performed MCR and imaged the fluorescently tagged probes by epifluorescence microscopy. As shown in Figure 3 A and B, a significant fluorescence signal was observed on the surface.

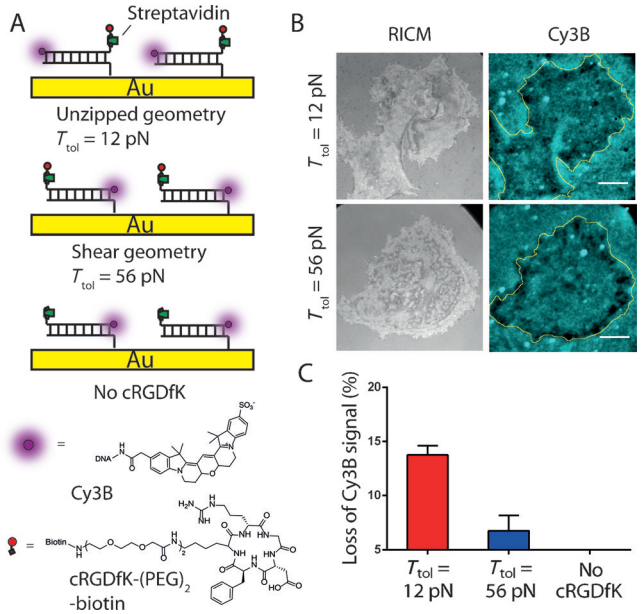

Figure 2. A) Schematic of mechanically labile duplexes used to study integrin-mediated forces. B) Representative RICM and fluorescence images of cells cultured on T_{tol} = 12 pN and T_{tol} = 56 pN surfaces. The negative signal observed in the Cy3B channel colocalized with cell adhesion patterns in RICM. Yellow line shows the cell edge as determined from RICM. Scale bars = 10 μm. C) Plot quantifying loss of Cy3B fluorescence, which indicates mechanical DNA denaturation (n = 10 cells).

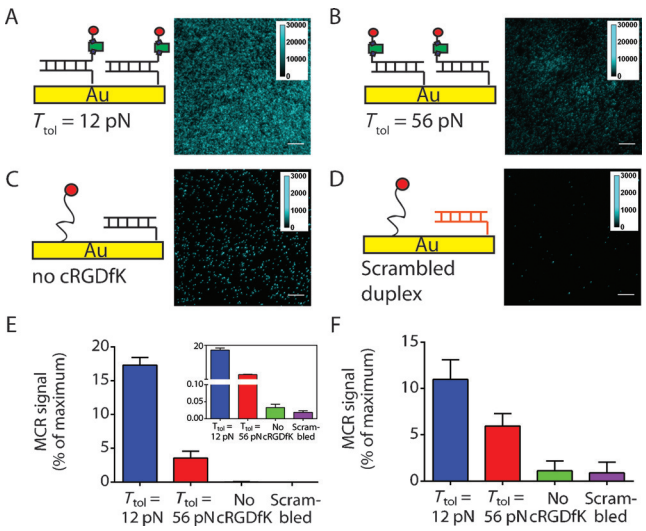

Figure 3. MCR to report integrin forces. Schematic and representative fluorescence images of A) duplexes with T_{tol} = 12 pN, B) T_{tol} = 56 pN, C) duplexes lacking the cRGDfK peptide, and D) scrambled duplexes. E) Bar graph showing the average MCR signal from 30 different images from three independent samples. Error bars represent the S.E.M. of the results. F) Bar graph showing the intensity of the eluent following release of FISH probes from the surfaces and detected by a microplate reader. Error bars represent the S.E.M. of the results from three independent experiments. Scale bars = 10 μm.

Therefore, primer amplification can readily be used to detect integrin-driven denaturation of blocked primers. Note that MCR was performed in standard conditions (Tris-OAc (20 mM), KOAc (50 mM), $Mg(OAc)_2$ (10 mM), BSA (100 μg mL^{-1}), pH 7.9), as media compatible with cells (such as DMEM, PBS, and HEPES) inhibit polymerase activity needed for MCR (Supporting Information, Figure S2). Therefore, cells are absent during readout, likely because of multiple washing and incubation steps in MCR buffer.

Controls using duplexes lacking cRGDfK (Figure 3C) and scrambled duplexes non-complementary to the template (Figure 3D) confirmed the specificity of MCR. In these controls, we doped the DNA surface with 10% (by incubation concentration) single-stranded DNA labeled with cRGDfK to mediate cell adhesion. The cell density was nearly identical on all the tested surfaces in Figure 3, indicating that the density of cRGDfK ligands was sufficient to trigger cell adhesion prior to MCR readout (Supporting Information, Figure S3). All controls showed low signal, approximately 150-fold lower than that generated by the 12 pN surface (Figure 3C and D). The background signal observed in Figure 3C is likely to arise from amplification of single-stranded primers exposed because of spontaneous dissociation of DNA duplexes. Confirming this result, we found an approximately 3% loss of fluorescently labeled DNA duplexes from the surface when incubated in cell imaging media for 3 hrs at 37 °C (Supporting Information, Figure S4).

The bar graphs in Figures 3E and F show the results of quantifying the MCR signal using imaging-based, and plate reader-based readouts, respectively. For plate reader-based readout, the bound FISH probes were released by dehybridization with nanopure water, and then transferred to a 96-well plate where fluorescence was quantified. Importantly, the fluorescence intensity was normalized to the maximum MCR signal obtained from a monolayer of primer (ca. 3.5×10^4 primers per μm^2 (Supporting Information, Supplementary Note 1), which is consistent with the literature precedent[16]) prepared in the same batch. The differences between image-based and plate-reader based readouts are likely because of differential levels of background and sensitivity; the image-based readout is likely to be more sensitive. The 12 pN duplex showed a roughly five-fold and 2.7-fold greater signal than that of the 56 pN duplex in Figures 3E and 3F, respectively, consistent with the mechanically induced dehybridization data in Figure 2.

Subsequently, we demonstrated suitability of the MCR amplification reaction in drug screening by measuring the effect of a drug on integrin mechanics rather than cell viability. We investigated the non-muscle myosin II inhibitor blebbistatin, which diminishes myosin contractility and thus reduces forces transmitted by focal adhesions. We pretreated NIH/3T3 cells with a range of blebbistatin concentrations (10 nM–10 μM) for 15 min and then incubated the cells onto the surface with the 12 pN duplexes for 1 h, which was then followed by MCR readout. Brightfield imaging indicated that cells become more rounded with increasing drug dose (Supporting Information, Figure S5). This observation is confirmed by *F*-actin staining, which showed more disorganized and shorter actin filaments at the highest blebbistatin doses (Figure 4A). Correspondingly, the MCR signal displayed a dose-dependent relationship, where the highest blebbistatin concentrations generated the lowest MCR signal

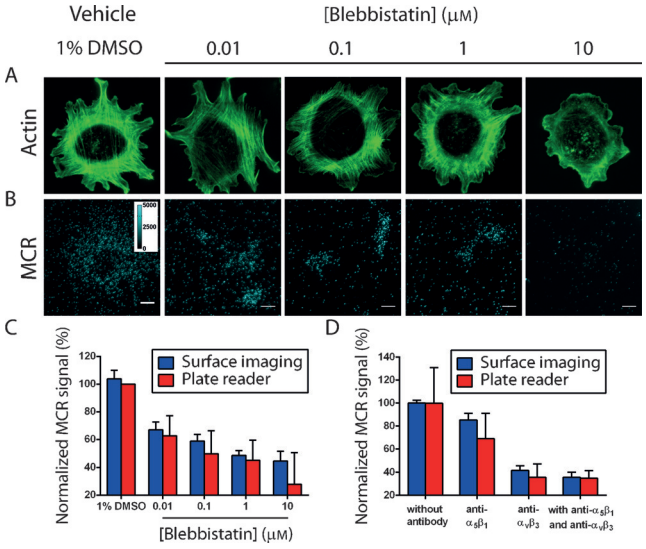

Figure 4. Representative fluorescence images showing A) *F*-actin staining and B) MCR signal for NIH/3T3 cells treated with increasing concentrations of blebbistatin (0.01–10 μM). C) Bar chart showing the MCR signal in response to increasing concentration of blebbistatin. D) Bar chart quantifying MCR signal in the presence of anti-$\alpha_5\beta_1$, anti-$\alpha_v\beta_3$, or both antibodies, relative to the sample without antibodies. Error bars represent the S.E.M. from $n=30$ images from three independent samples in surface imaging readout, and $n=3$ independent samples for plate reader based readout. Scale bars = 10 μm.

(Figure 4B and C). The MCR signal is a direct readout of integrin tension, measuring the dose-dependent dissipation of actomyosin contractile forces.

To further highlight the utility of MCR, we measured the MCR signal on the 12 pN duplex surfaces in response to inhibiting different integrin subtypes. The two major integrin subtypes mediating adhesion of NIH/3T3 fibroblasts are $\alpha_v\beta_3$ and $\alpha_5\beta_1$ that display divergent cellular functions.[17] In surface-based imaging, anti-$\alpha_v\beta_3$ antibody treatment reduced the MCR signal by $59.6\pm4.1\%$, while anti-$\alpha_5\beta_1$ antibody treatment reduced the MCR signal by $14.6\pm5.6\%$ (Figure 4D, blue bars; Supporting Information, Figure S6). Incubation with both antibodies led to the greatest reduction in MCR signal ($64.4\pm4.3\%$). Plate reader measurement showed a similar trend (Figure 4D, red bars). The differential MCR signal following antibody blocking is likely because of a number of factors. First, $\alpha_v\beta_3$ integrins play a more important role in mediating the adhesion of fibroblasts.[18] Second, the experiment is performed after 1 h of cell incubation, and $\alpha_v\beta_3$ integrins are thought to initiate cell adhesion.[19] Finally, $\alpha_v\beta_3$ integrins show higher affinity toward the cRGDfK ligand ($K_d\approx$ nM) compared to that of $\alpha_5\beta_1$.[20] Taken together, we demonstrate the first example of screening drugs that target cellular mechanics using a catalytic amplification assay.

Acknowledgements

K.S. is thankful for financial support from the NIH (R01-GM097399), the Alfred P. Sloan Research Fellowship, the Camille-Dreyfus Teacher-Scholar Award, and the NSF CAREER Award (1350829).

Keywords: drug screening · integrins · mechanically induced catalytic amplification · receptor-mediated forces · rolling circle amplification

How to cite: *Angew. Chem. Int. Ed.* **2016**, *55*, 5488–5492
Angew. Chem. **2016**, *128*, 5578–5582

[1] a) A. W. Orr, B. P. Helmke, B. R. Blackman, M. A. Schwartz, *Dev. Cell* **2006**, *10*, 11–20; b) D. E. Ingber, *FASEB J.* **2006**, *20*, 811–827; c) D. E. Jaalouk, J. Lammerding, *Nat. Rev. Mol. Cell Biol.* **2009**, *10*, 63–73; d) Z. Liu, Y. Liu, Y. Chang, H. R. Seyf, A. Henry, A. L. Mattheyses, K. Yehl, Y. Zhang, Z. Huang, K. Salaita, *Nat. Methods* **2016**, *13*, 143–146.

[2] J. N. Brantley, C. B. Bailey, K. M. Wiggins, A. T. Keatinge-Clay, C. W. Bielawski, *Polym. Chem.* **2013**, *4*, 3916–3928.

[3] a) D. R. Stabley, C. Jurchenko, S. S. Marshall, K. S. Salaita, *Nat. Methods* **2012**, *9*, 64–67; b) C. Jurchenko, K. S. Salaita, *Mol. Cell. Biol.* **2015**, *35*, 0.

[4] C. Jurchenko, Y. Chang, Y. Narui, Y. Zhang, K. S. Salaita, *Biophys. J.* **2014**, *106*, 1436–1446.

[5] a) B. L. Blakely, C. E. Dumelin, B. Trappmann, L. M. McGregor, C. K. Choi, P. C. Anthony, V. K. Duesterberg, B. M. Baker, S. M. Block, D. R. Liu, C. S. Chen, *Nat. Methods* **2014**, *11*, 1229–1232; b) Y. Zhang, C. Ge, C. Zhu, K. Salaita, *Nat. Commun.* **2014**, *5*, 5167.

[6] a) M. Morimatsu, A. H. Mekhdjian, A. S. Adhikari, A. R. Dunn, *Nano Lett.* **2013**, *13*, 3985–3989; b) M. Morimatsu, A. H. Mekhdjian, A. C. Chang, S. J. Tan, A. R. Dunn, *Nano Lett.* **2015**, *15*, 2220–2228.

[7] K. Galior, Y. Liu, K. Yehl, S. Vivek, K. Salaita, *Nano Lett.* **2016**, *16*, 341–348.

[8] a) Y. Liu, K. Yehl, Y. Narui, K. Salaita, *J. Am. Chem. Soc.* **2013**, *135*, 5320–5323; b) Y. Liu, R. Medda, Z. Liu, K. Galior, K. Yehl, J. P. Spatz, E. A. Cavalcanti-Adam, K. Salaita, *Nano Lett.* **2014**, *14*, 5539–5546; c) Y. Chang, Z. Liu, Y. Zhang, K. Galior, J. Yang, K. Salaita, *J. Am. Chem. Soc.* **2016**, *138*, 2901–2904.

[9] a) G. J. L. Wuite, S. B. Smith, M. Young, D. Keller, C. Bustamante, *Nature* **2000**, *404*, 103–106; b) B. Maier, D. Bensimon, V. Croquette, *Proc. Natl. Acad. Sci. USA* **2000**, *97*, 12002–12007.

[10] a) D. Mertz, C. Vogt, J. Hemmerle, J. Mutterer, V. Ball, J.-C. Voegel, P. Schaaf, P. Lavalle, *Nat. Mater.* **2009**, *8*, 731–735; b) X. He, M. Aizenberg, O. Kuksenok, L. D. Zarzar, A. Shastri, A. C. Balazs, J. Aizenberg, *Nature* **2012**, *487*, 214–218.

[11] a) X. Wang, T. Ha, *Science* **2013**, *340*, 991–994; b) F. Chowdhury, I. T. S. Li, B. J. Leslie, S. Doganay, R. Singh, X. Wang, J. Seong, S.-H. Lee, S. Park, N. Wang, T. Ha, *Integr. Biol.* **2015**, *7*, 1265–1271.

[12] a) M. M. Ali, F. Li, Z. Zhang, K. Zhang, D.-K. Kang, J. A. Ankrum, X. C. Le, W. Zhao, *Chem. Soc. Rev.* **2014**, *43*, 3324–3341; b) Y. Zhao, F. Chen, Q. Li, L. Wang, C. Fan, *Chem. Rev.* **2015**, *115*, 12491–12545.

[13] a) C. Larsson, I. Grundberg, O. Soderberg, M. Nilsson, *Nat. Methods* **2010**, *7*, 395–397; b) R. Ke, M. Mignardi, A. Pacureanu, J. Svedlund, J. Botling, C. Wahlby, M. Nilsson, *Nat. Methods* **2013**, *10*, 857–860; c) C. Russell, K. Welch, J. Jarvius, Y. Cai, R. Brucas, F. Nikolajeff, P. Svedlindh, M. Nilsson, *ACS Nano* **2014**, *8*, 1147–1153.

[14] K. Yehl, A. Mugler, S. Vivek, Y. Liu, Y. Zhang, M. Fan, E. R. Weeks, K. Salaita, *Nat. Nanotechnol.* **2016**, *11*, 184–190.

[15] T. D. Ross, B. G. Coon, S. Yun, N. Baeyens, K. Tanaka, M. Ouyang, M. A. Schwartz, *Curr. Opin. Cell Biol.* **2013**, *25*, 613–618.

[16] A. W. Peterson, R. J. Heaton, R. M. Georgiadis, *Nucleic Acids Res.* **2001**, *29*, 5163 – 5168.
[17] P. Roca-Cusachs, N. C. Gauthier, A. del Rio, M. P. Sheetz, *Proc. Natl. Acad. Sci. USA* **2009**, *106*, 16245 – 16250.
[18] S. P. Massia, J. A. Hubbell, *J. Cell Biol.* **1991**, *114*, 1089 – 1100.
[19] E. Zamir, M. Katz, Y. Posen, N. Erez, K. M. Yamada, B.-Z. Katz, S. Lin, D. C. Lin, A. Bershadsky, Z. Kam, B. Geiger, *Nat. Cell Biol.* **2000**, *2*, 191 – 196.
[20] M. Schottelius, B. Laufer, H. Kessler, H.-J. Wester, *Acc. Chem. Res.* **2009**, *42*, 969 – 980.

Received: January 12, 2016
Published online: April 1, 2016

